Research and Development Technical Report
SLCET-TR-91-35

LITHIUM RECHARGEABLE CELL WITH A POLYMER CATHODE

Charles W. Walker, Jr.
ELECTRONICS TECHNOLOGY AND DEVICES LABORATORY

NOVEMBER 1991

DISTRIBUTION STATEMENT

Approved for public release;
Distribution is unlimited.

U.S. ARMY LABORATORY COMMAND

Electronics Technology and Devices Laboratory
Fort Monmouth, NJ 07703-5601

NOTICES

Disclaimers

The findings in this report are not to be construed as an official Department of the Army position, unless so designated by other authorized documents.

The citation of trade names and names of manufacturers in this report is not to be construed as official Government indorsement or approval of commercial products or services referenced herein.

REPORT DOCUMENTATION PAGE

Form Approved
OMB No. 0704-0188

1. AGENCY USE ONLY (Leave blank)	2. REPORT DATE	3. REPORT TYPE AND DATES COVERED
	Nov 1991	Final Report Oct 89 to Jan 91

4. TITLE AND SUBTITLE

LITHIUM RECHARGEABLE CELL WITH A POLYMER CATHODE

5. FUNDING NUMBERS

6. AUTHOR(S)

Charles W. Walker, Jr.

7. PERFORMING ORGANIZATION NAME(S) AND ADDRESS(ES)

U.S. Army Laboratory Command (LABCOM)
Electronics Technology and Devices Laboratory (ETDL)
ATTN: SLCET-PR
Fort Monmouth, NJ 07703-5601

8. PERFORMING ORGANIZATION REPORT NUMBER

SLCET-TR-91-35

9. SPONSORING/MONITORING AGENCY NAME(S) AND ADDRESS(ES)

10. SPONSORING/MONITORING AGENCY REPORT NUMBER

11. SUPPLEMENTARY NOTES

12a. DISTRIBUTION/AVAILABILITY STATEMENT

Approved for public release; distribution is unlimited.

12b. DISTRIBUTION CODE

13. ABSTRACT (Maximum 200 words)

Thin films of electropolymerized poly 3-methylthiophene (PMT) were used as a rechargeable cathode in $Li(SO_2)_3AlCl_4$ electrolyte. Capacity was superior to porous carbon electrodes of like thickness. Pulse power levels of 2 W cm^{-2} were achieved, and high rate constant current pulses of four-second duration were reproducible over many cycles. Cells could be recharged at potentials below 4.0 V, minimizing the formation of chlorine and thereby diminishing the capacity for corrosion.
As a primary cell, greater discharge capacity was obtained with thionyl chloride and sulfuryl chloride electrolytes.
Since PMT becomes electrically insulating in the reduced state, this could be used as a built-in safety feature to avert the hazards associated with abuse over-discharge.

14. SUBJECT TERMS

batteries; lithium; polymer; thiophenes; cathodes; carbon; sulfur dioxide; thionyl chloride

15. NUMBER OF PAGES

35

16. PRICE CODE

17. SECURITY CLASSIFICATION OF REPORT	18. SECURITY CLASSIFICATION OF THIS PAGE	19. SECURITY CLASSIFICATION OF ABSTRACT	20. LIMITATION OF ABSTRACT
UNCLASSIFIED	UNCLASSIFIED	UNCLASSIFIED	UL

GENERAL INSTRUCTIONS FOR COMPLETING SF 298

The Report Documentation Page (RDP) is used in announcing and cataloging reports. It is important that this information be consistent with the rest of the report, particularly the cover and title page. Instructions for filling in each block of the form follow. It is important to ***stay within the lines*** to meet ***optical scanning requirements***.

Block 1. Agency Use Only *(Leave blank)*.

Block 2. Report Date. Full publication date including day, month, and year, if available (e.g. 1 Jan 88). Must cite at least the year.

Block 3. Type of Report and Dates Covered. State whether report is interim, final, etc. If applicable, enter inclusive report dates (e.g. 10 Jun 87 - 30 Jun 88).

Block 4. Title and Subtitle. A title is taken from the part of the report that provides the most meaningful and complete information. When a report is prepared in more than one volume, repeat the primary title, add volume number, and include subtitle for the specific volume. On classified documents enter the title classification in parentheses.

Block 5. Funding Numbers. To include contract and grant numbers; may include program element number(s), project number(s), task number(s), and work unit number(s). Use the following labels:

C	- Contract	PR	- Project
G	- Grant	TA	- Task
PE	- Program Element	WU	- Work Unit Accession No.

Block 6. Author(s). Name(s) of person(s) responsible for writing the report, performing the research, or credited with the content of the report. If editor or compiler, this should follow the name(s).

Block 7. Performing Organization Name(s) and Address(es). Self-explanatory.

Block 8. Performing Organization Report Number. Enter the unique alphanumeric report number(s) assigned by the organization performing the report.

Block 9. Sponsoring/Monitoring Agency Name(s) and Address(es) Self-explanatory.

Block 10. Sponsoring/Monitoring Agency Report Number *(If known)*

Block 11. Supplementary Notes. Enter information not included elsewhere such as: Prepared in cooperation with , Trans. of...; To be published in.... When a report is revised, include a statement whether the new report supersedes or supplements the older report.

Block 12a. Distribution/Availability Statement. Denotes public availability or limitations. Cite any availability to the public. Enter additional limitations or special markings in all capitals (e.g. NOFORN, REL, ITAR).

- **DOD** - See DoDD 5230.24, "Distribution Statements on Technical Documents."
- **DOE** - See authorities.
- **NASA** - See Handbook NHB 2200.2.
- **NTIS** - Leave blank.

Block 12b. Distribution Code.

- **DOD** - Leave blank.
- **DOE** - Enter DOE distribution categories from the Standard Distribution for Unclassified Scientific and Technical Reports.
- **NASA** - Leave blank.
- **NTIS** - Leave blank.

Block 13. Abstract. Include a brief *(Maximum 200 words)* factual summary of the most significant information contained in the report.

Block 14. Subject Terms. Keywords or phrases identifying major subjects in the report.

Block 15. Number of Pages. Enter the total number of pages.

Block 16. Price Code. Enter appropriate price code *(NTIS only)*.

Blocks 17. - 19. Security Classifications. Self-explanatory. Enter U.S. Security Classification in accordance with U.S. Security Regulations (i.e., UNCLASSIFIED). If form contains classified information, stamp classification on the top and bottom of the page

Block 20. Limitation of Abstract. This block must be completed to assign a limitation to the abstract. Enter either UL (unlimited) or SAR (same as report). An entry in this block is necessary if the abstract is to be limited. If blank, the abstract is assumed to be unlimited.

CONTENTS

FIGURES

TABLES

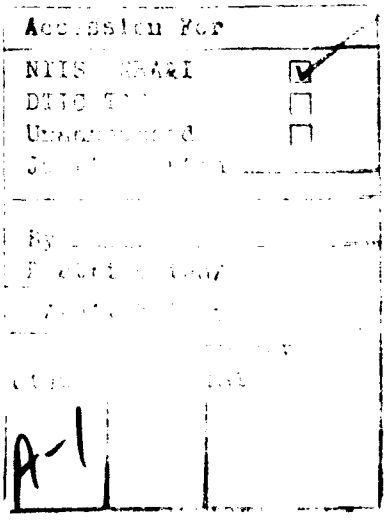

INTRODUCTION

The search for man-portable power sources with high energy density and power never ceases as the development of new technologies demand increased energy. There is also impetus to extend the service life of batteries used in existing equipment. Guidelines include a system that is rechargeable, has good storage in the charged state, is lightweight, and safe to operate under a variety of load conditions and temperatures.

To fulfill these requirements, lithium rechargeable cells containing organic and inorganic electrolytes have been studied for some time. The (rechargeable) inorganic electrolyte receiving the most consideration has been based on sulfur dioxide. Because electrolyte conductivity is high (on the order of 1×10^{-1} S cm^{-1}), this system allows high rate discharge capability. Most work with SO_2 has involved cathodes composed of carbon black, as are utilized in primary batteries.

Using $Li(SO_2)_3AlCl_4$ electrolyte, Mammonne and Binder (1) found evidence that lithium dithionite ($Li_2S_2O_4$) was formed on discharge, and proposed that cell recharge occurred via oxidation of $AlCl_4^-$ to form $AlCl_3$ and Cl_2. The formed Cl_2 would chemically oxidize $Li_2S_2O_4$ while $AlCl_3$ would recombine as follows

$$Cl_2 + Li_2S_2O_4 \rightarrow 2SO_2 + 2LiCl \quad [1]$$

$$2LiCl + 2AlCl_3 \rightarrow 2LiAlCl_4 \quad [2]$$

A more widely held view of the cell chemistry was given by Dey et al. (2). Discharge products at the cathode included LiCl and a carbon-electrolyte complex via the cell reaction

$$3Li + 3SO_2 + LiAlCl_4 + C_x \leftrightarrow LiCl\text{-}Al\left(\begin{array}{l} O\text{-}S\text{-}O\text{-}C \\ O\text{-}S\text{-}O\text{-}C \\ O\text{-}S\text{-}O\text{-}C \end{array}\right) + 3LiCl \quad [3]$$

During charge, $AlCl_4^-$ is oxidized to Cl_2 and $AlCl_3$, and Li^+ is reduced to metallic lithium. Protection from overcharge is provided by recombination of the redox products of $LiAlCl_4$ by

$$Cl_2 + 2Li \rightarrow 2LiCl \quad [4]$$

then

$$2LiCl + 2AlCl_3 \rightarrow 2LiAlCl_4 \quad [5]$$

However, the reaction schemes proposed by both groups involve formation of Cl_2 during charge, and this increases rates of lithium corrosion and separator degradation.

We chose to study cathode materials other than carbon blacks, and hoped to reduce cell charging potential to avoid the formation of chlorine. The material we report on here is an electrically conductive polymer, poly 3-methylthiophene (PMT).

Early studies of conductive polymers began with poly(acetylene). Since then, many polymers have been explored, especially those containing aromatic ring structures, like PMT. An attractive feature of PMT is that it is stable in air, and can be electrochemically formed as an extremely thin film, with surface area and electrical conductivity controlled by the conditions under which electropolymerization is carried out. When oxidized (doped state), PMT is positively charged, and is electrically neutralized by anions from solution entering the matrix. In this state, PMT reportedly has an electrical conductivity in the range of 10-2000 S cm^{-1} (3-5). Factors influencing conductivity are the choice of dopant anion, film thickness, and level of doping. Upon reduction of the polymer to the neutral state, anions diffuse from the polymer matrix back into the electrolyte, and the polymer becomes electrically insulating.

Using a PMT cathode in a Li/SO_2 cell, we studied charge/discharge cycling characteristics and pluse power capability. Additionally, we also studied high rate discharge of PMT electrodes in sulfuryl chloride (SO_2Cl_2) and thionyl chloride ($SOCl_2$) electrolytes for possible application in a reserve cell.

EXPERIMENTAL

Electropolymerization of PMT- PMT was prepared in a 125 ml European style flask (Ace Glass) using a 1 cm^2 platinum flag counterelectrode, a saturated sodium calomel reference electrode, and a platinum or glassy carbon rod working electrode. Glassy carbon and platinum rods (0.071 cm^2 cross section) were polished to a mirror finish with 0.1 micron alumina/water paste. The rod was sheathed in heat-shrinkable Teflon so as to expose only the 0.071 cm^{-2} cross-sectional area at the end of the rod. The cell was also fitted with a glass tube for bubbling gas and a gas outlet. The cell was flooded with electrolyte containing 0.1 M 3-methylthiophene monomer (Sigma Chemical, 99+%) and 0.1 M tetrabutylammonium tetrafluoroborate (Alpha), in distilled acetonitrile (Fisher) while bubbling ultra high purity dry argon. Ultra high-purity dry argon was also bubbled through the electrolyte prior to electropolymerization to remove oxygen.

PMT polymerization occurred when the potential (working vs reference) was $\geq$1.5 V. Constant current polymerization carried out at 7 mA cm^{-2} provided a potential between 1.5 and 1.6 V and produced visually uniform films which strongly adhered to the substrate. PMT-coated rods were rinsed in acetonitrile and dried under vacuum at 50°C. In the oxidized (doped, conductive)

state PMT is blue in color, while reduced (undoped, electrically insulating) PMT is red. A 0.41 μm thick film (measured by SEM) was formed by passing 0.25 C cm^{-2} (deposition rate of 0.61 C cm^{-2} μm^{-1}). Thicker films could not be produced at 7 mA cm^{-2} since during polymerization the potential slowly fell below 1.5 V. Higher currents (10 mA cm^{-2}) produced a mossy, dendritic, nonadherent films. However, thick adherent films could be fabricated at 10 mA cm^{-2} by a pulse deposition process. This was accomplished by passing 1.25 C cm^{-2} in five cycles (0.25 C cm^{-2} per cycle) with 5 minute rest periods (at open circuit) between cycles to re-establish equilibrium conditions. This procedure built up a 1.4 μm thick PMT film.

Based on the number of coulombs passed, to a first approximation (assuming 100% plating efficiency), a maximum of 4.52×10^{-5} g of 3-methylthiophene was deposited on the substrate.

Porous carbon electrodes - Two types of porous carbon cathodes were also studied for comparison with PMT. The first type was a relatively thick (800 μm) "conventional" electrode consisting of a mixture of Shawinigan and Ketjen black with 10% PTFE binder on a nickel grid as previously described (6).

The other type of carbon cathode was a miniature porous electrode (7) similar in size to the PMT electrodes. It contained no binder and was 0.098 cm^2 and between 20 and 50 μm thick. This electrode was constructed by coating the exposed cross-sectional end (0.098 cm^2) of a Teflon-sheathed glassy carbon rod with conducting silver epoxy (AESAR Mattheylec A-500). Prior to curing, the epoxy-covered end was pressed into a tube containing Shawinigan carbon and then removed. After drying overnight under vacuum at 50°C, excess carbon was removed by gentle agitation in a water-acetone solution and dried again. The rod was lightly rubbed across a piece of paper to smooth out the contour.

Electrolyte preparation - $Li(SO_2)_3AlCl_4$ electrolyte was prepared with anhydrous $LiAlCl_4$ (Anderson Physics) and excess dry liquid SO_2 (Matheson) by combining them in an evacuated Teflon cell (able to withstand pressure). After dissolution of the salt, excess SO_2 was slowly bled off through a bubbler containing halocarbon oil. The resultant electrolyte was between 3 and 3.5 SO_2 molecules per $LiAlCl_4$ molecule as measured by weight. Anhydrous LiCl was added to scavenge any excess $AlCl_3$ and ensure a neutral electrolyte.

Electrolytes containing $SOCl_2$ and SO_2Cl_2 were prepared after distilling each solvent over lithium ribbon while bubbling dry argon, and by dissolving anhydrous $LiAlCl_4$ to form a 1.0 M solution. Excess anhydrous LiCl was then added to ensure solution neutrality.

Cell configuration - Cell studies were performed in a 125 ml European flask containing 20 ml of electrolyte, a large lithium anode, and lithium reference electrode. A PAR model 273 or Model 173 potentiostat/galvanostat with a Model 276 plug-in interface was used in conjunction with Hewlett Packard HP 80 Series computers to control all experiments and electropolymerization of PMT. Cyclic voltammetry was performed with a PAR Model 175 Universal Programmer. All experiments were conducted at 25°C.

RESULTS AND DISCUSSION

Scanning electron microscopy (SEM) - SEM photographs of 0.41 μm and 1.4 μm thick PMT films at 5000x showed a compact layer of polymer attached to the substrate. Upon this layer, the 0.41 μm film had nodules measuring 1 μm in diameter uniformly spaced approximately 1 μm apart. The 1.4 μm film had larger nodules (1-2 μm diameter) entirely covering the surface of the compact layer. The total surface area of the 1.4 μm film was clearly much higher than that of the 0.41 μm film. This was expected since it is well known that increasing polymerization rate or growing successive layers increases surface area (5, 8-11). Based on the cross-sectional area and thickness, the 1.4 μm thick PMT had a volume of 9.95×10^{-6} cm^3.

Surface Area Analysis - A BET gas adsorption surface area analysis was performed (Micromeritics, Norcross, GA) on a 120 mg sample of PMT collected from several films prepared at the 10 mA cm^{-2} rate. The single point analysis revealed a surface area of 4.13 m^2 g^{-1}. This is much lower than the surface area of carbon blacks, which range from 60 to 1500 m^2 g^{-1}.

Cyclic Voltammetry - Cyclic voltammograms of PMT doped with BF_4^- showed a large reduction peak (in SO_2 electrolyte) at 2.74 V (1000 mV s^{-1}) which agreed with previous findings (12). Sulfur dioxide reduction was shifted from the expected value of 2.9 V observed at glassy carbon electrodes (1) as explained by Mammone and Binder (12). The shift in reduction potential indicates that the nature of the discharge product is dependent on the cathode substrate. When scanning anodically at 100 mV s^{-1}, a large oxidation peak was observed at 3.74-3.78 V. It was therefore expected that cell recharge could be accomplished at 3.8 V.

Cl_2 formation - The $Li(SO_2)_3AlCl_4$ electrolyte was studied to determine the amount of Cl_2 formed by the oxidation of $AlCl_4^-$ as cell potential was held at increasingly anodic potentials from 3.6 to 4.2 V. To maximize product formation, a "large" 1 cm^2 Teflon-bonded porous carbon electrode was used. Aliquots of electrolyte were withdrawn for UV-VIS spectroscopic analysis of chlorine. At 360 nm a shoulder assigned to Cl_2 appeared only in solutions held at 3.9 V and above. Strong absorbance by the electroyte in this region prevented quantitative analysis. The effects of dilution, loss of Cl_2 gas, and combination of Cl_2 with

SO_2 to form SO_2Cl_2 may have added further complications. Therefore, it was not possible to determine a charging potential below which there is no oxidation of $AlCl_4^-$ to form Cl_2 and $AlCl_3$. However, because no Cl_2 could be detected when the potential was held below 3.9 V, it was assumed that insignificant amounts of chlorine form below this potential. Corroborating evidence for this assumption is that oxidation of $AlCl_4^-$ to form Cl_2 in $LiAlCl_4$- based electrolytes containing either $SOCl_2$ or SO_2Cl_2 was found to occur at potentials greater than 4.1 V (13-14).

Theoretical Capacity - Discharge of PMT in $Li(SO_2)_3AlCl_4$ involves two processes, reduction (undoping) of the polymer and reduction of the electrolyte. The theoretical energy derived from polymer undoping alone can be calculated by

$$\frac{Ah}{kg} = \frac{(96480\ C\ F^{-1})\ (1000\ g\ kg^{-1})}{(g\ F^{-1})\ (3600\ s\ h^{-1})} = \frac{26800}{(g\ F^{-1})} \quad [6]$$

Writing the overall discharge reaction and solving for g F^{-1} by inserting the formula weights for the electroactive species we have

$$[(C_5H_4S^{+y})(AlCl_4^-)_y]_x + xy(Li) \rightarrow (C_5H_4S)_x + xy(LiAlCl_4) \quad [7]$$

$$g\ F^{-1} = \frac{x(C_5H_4S) + xy(LiAlCl_4)}{xy} \quad [8]$$

$$= \frac{x(96.15) + xy(175.7)}{xy} \quad [9]$$

$$= \frac{96.15}{y} + 175.7 \quad [10]$$

where "y" represents the percent doping.

Based on an optimistic doping level of 50% (y=0.5), we calculate a theoretical energy of 72.8 Ah kg^{-1} for fully undoping PMT. Using an operating load voltage of 3.1 V reported for constant current discharge in $Li(SO_2)_3AlCl_4$ electrolyte (15), we arrive at 225.7 Wh kg^{-1} (assuming we could achieve 100% undoping at this potential). A more realistic dopant level of 35% yields theoretical values of 59.5 Ah kg^{-1} and 184.5 Wh kg^{-1}. In fact, a dopant level of less than 50% would be preferred based on the work of Ofer, Crooks and Wrighton (16), who have determined that there is a potential window of high conductivity. As neutral (insulating) polymer is oxidized and dopant level is increased, a maximum in conductivity is attained beyond which conductivity decreases with further oxidation. They found that a maximum conductivity for PMT occurred at ≈0.3 electrons per repeat unit, and beyond ≈0.5 electrons per repeat unit thiophenes tended to decompose. Another indication arguing for doping levels of about 30% was shown by Kawai et al. (17) in studies with poly (3-

octylthiophene). They determined a coulombic efficiency of only 47% at a maximum doping level of 48.6%, whereas at a 33% doping level efficiency was 94%.

Cycling of PMT - When PMT is polymerized (in the acetonitrile-based electrolyte) it is doped with BF_4^- anions. As such, poor capacity was observed on discharge in a lithium cell containing $Li(SO_2)_3AlCl_4$ electrolyte. With cycling, BF_4^- exchanges with $AlCl_4^-$ from the electrolyte, and discharge capacity significantly improves. Poor capacity of the virgin film could have been due to BF_4^- leaking out of the polymer matrix prior to the initial discharge, causing a partially undoped polymer. It is also possible that electrical conductivity increases when PMT is doped with $AlCl_4^-$ anions. It was presumed that capacity also improved due to swelling of the polymer. Others have commonly observed better performance after a "break-in" period as well. Kawai et al. (17) observed an increase in cycling efficiency with cycle number for various poly (3-alkylthiophenes). They attributed this to two effects; and accumulation of dopant ions trapped in the polymer, and secondly, a structural change of the polymer matrix which allows dopant ions to migrate more easily within the polymer. Pern and Frank (18) also had evidence of these two effects based on data obtained for PMT. Likewise, we presume that the polymer lattice of $AlCl_4^-$-doped PMT is expanded, facilitating diffusion of ions and creating more surface area for contact with the electrolyte. This would explain the increase in discharge capacities seen during the first few cycles. As a result of this observation, the usual method of treatment was to first undope BF_4^- from the polymer in $Li(SO_2)_3AlCl_4$ electrolyte by holding the potential at 3.0 V (relative to lithium) and then doping with $AlCl_4^-$ at either 3.7 or 3.8 V constant potential. By recharging below 3.9 V we assumed insignificant amounts of Cl_2 were formed by the oxidation of $AlCl_4^-$. This procedure resulted in good capacity on first discharge. After standing overnight, open-circuit voltage (OCV) of PMT doped with $AlCl_4^-$ was 3.4 V (relative to lithium).

Performance of PMT on first discharge was compared to bare polished platinum and polished glassy carbon as well as to the miniature porous carbon electrodes (Figure 1, Table I). At a discharge rate of 0.05 mA cm^{-2} to a 2.0 V cutoff, only 1 to 3 minutes of capacity was obtained with glassy carbon electrodes (not shown). Smooth platinum (with a surface are similar to glassy carbon) also gave little capacity. The ≈25 fm thick porous carbon electrodes gave longer capacity, reflecting increased surface area and volume. Thicker (≈50 μm) porous carbon electrodes ran for about 200 min. By comparison, the first discharge of 0.41 μm PMT ran over 100 min, while thicker (1.4 μm) films ran for nearly 900 min. The 1.4 μm thick PMT is only about 3.5 times thicker than the thinner (0.41 μm) film, but the discharge time is nearly nine times greater. Although thicker films provided more capacity, constant potential recharge

at 3.8 V took much longer since ion diffusion occurred through a thicker film. Reasons for the extraordinary capacity could possibly be explained in part by dissolution of discharge product (discussed later) or by an alternate discharge mechanism and reduction products. It is also conceivable that PMT could act as a catalytic surface, or that reduction products do not firmly attach to PMT and tend to fall away from the electrode.

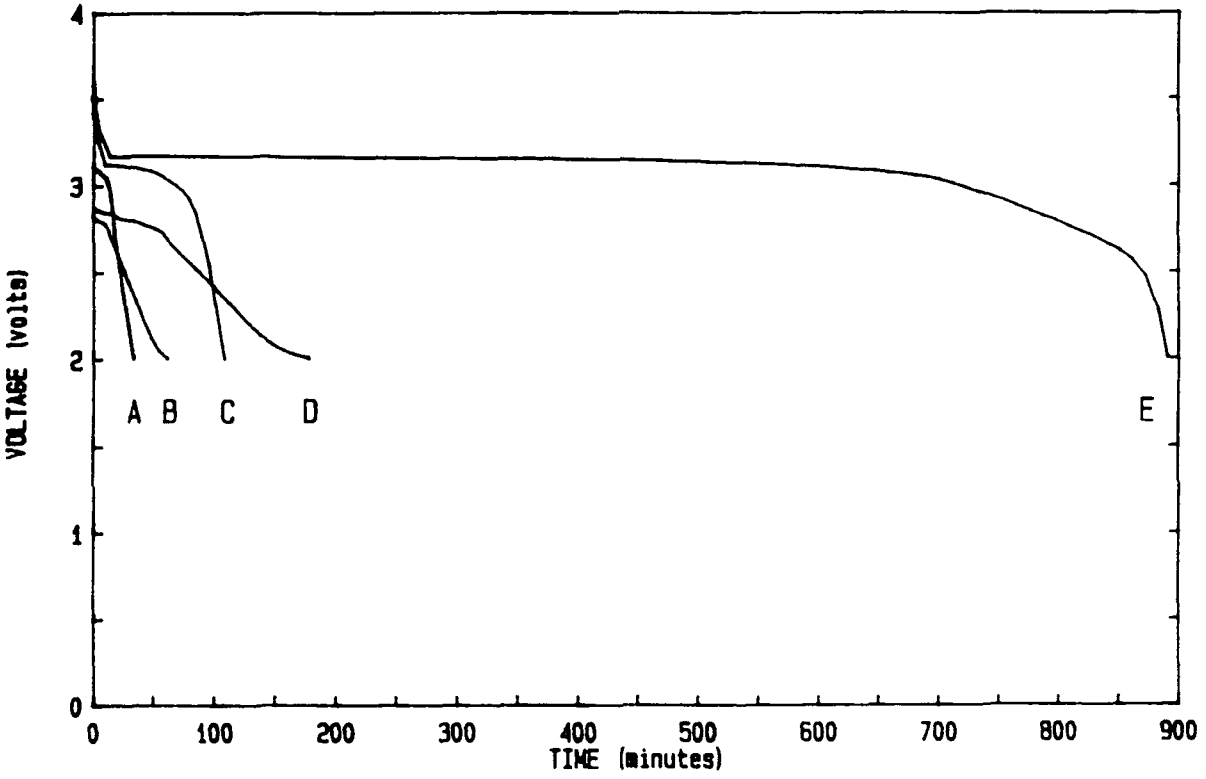

Figure 1. Cathode capacity comparison at 0.05 mA cm^{-2} rate in $Li(SO_2)_3AlCl_4$ electrolyte. Smooth platinum (A), ≈25 μm thick Shawinigan carbon (B), 0.41 μm thick PMT (C), ≈50 μm thick Shawinigan carbon (D), 1.4 μm thick PMT (E).

TABLE I.

Cathode performance in $Li(SO_2)_3AlCl_4$ electrolyte at 0.05 mA cm^{-2}.

Cathode type	Thickness μm	Discharge rate mA cm^{-2}	Ah cm^{-2}	Ah cm^{-3}	Cycle Number
PMT	0.41	0.05	$9.1x10^{-5}$	2.21	1
PMT	1.4	0.05	$7.4x10^{-4}$	5.30	1
Shawin[a]	25	0.05	$5.2x10^{-5}$	0.021	1
Shawin[a]	50	0.05	$1.5x10^{-4}$	0.030	1

[a] Miniature (0.098 cm^2) Shawinigan carbon electrodes as described in text.

In addition to electrolyte reduction, a small contribution to the total charge delivered by PMT is from polymer undoping, but this is small by comparison and cannot account for the high capacities observed.

Since the surface area of PMT was determined to be only 4.13 m^2 g^{-1}, good performance of PMT cathodes cannot be attributed to a high surface area. Because surface area of Shawinigan is 60 m^2 g^{-1}, we expected the porous carbon cathodes to out-perform PMT electrodes. In fact, the miniature carbon cathodes had volumetric energy densities lower than expected based on those normally observed for PTFE-bonded carbon cathodes. Since these miniature electrodes contained no binder, they may have had a collapsed structure that could account for the decrease in capacity.

Capacities of PMT films discharge at 1 mA cm^{-2} to a 2 V cutoff are shown in Figure 2 and Table II. Recharge was accomplished by holding the cell potential at 3.8 V and monitoring the coulombs passed, terminating when the charge removed during discharge was replaced. The third and seventh discharges are shown for 0.41 μm thick PMT and the first discharge of 1.4 μm film. Capacity usually improved over the first few cycles (exemplified by the 0.41 μm thick film) as the polymer swelled and doping levels of $AlCl_4^-$ increased. Figure 3 illustrates this point even more dramatically, showing the first, third, and fourth discharges of 1.4 μm thick PMT. The first discharge was performed without first undoping BF_4^- (and doping $AlCl_4^-$) in order to demonstrate the benefit of condition

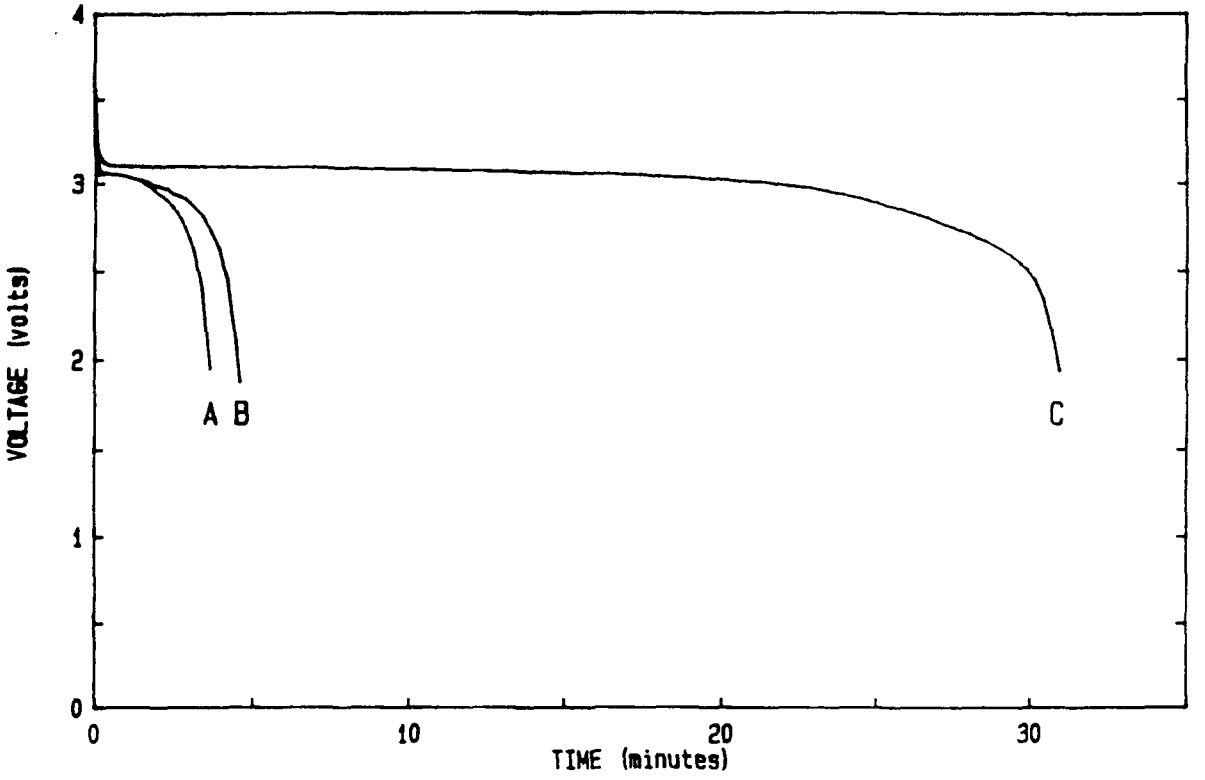

Figure 2. Capacity of PMT for 1 mA cm^{-2} discharge in $Li(SO_2)_3AlCl_4$ electrolyte. Curve (A) shows the third and curve (B) the seventh discharge of 0.41 μm thick PMT recharged at 3.8 V. Curve (C) is the first discharge of 1.4 μm thick PMT.

TABLE II.

Cathode performance in $Li(SO_2)_3AlCl_4$ at various discharge rates.

Cathode type	Thickness μm	Discharge rate mA cm^{-2}	Ah cm^{-2}	Ah cm^{-3}	Cycle Number
PMT	0.41	0.1	$4.3x10^{-5}$	1.04	1
PMT	0.41	0.1	$6.1X10^{-5}$	1.49	3
PMT	1.4	0.1	$3.2X10^{-4}$	2.32	1
PMT	1.4	0.1	$2.6X10^{-4}$	1.87	5
PMT	0.41	0.5	$7.2x10^{-5}$	1.77	1
PMT	0.41	0.5	$8.8x10^{-5}$	2.15	2
PMT	0.41	1.0	$6.2x10^{-5}$	1.51	3
PMT	0.41	1.0	$7.7x10^{-5}$	1.87	7

TABLE II (Cont)

Cathode type	Thickness μm	Discharge rate mA cm^{-2}	Ah cm^{-2}	Ah cm^{-3}	Cycle Number
PMT[a]	1.4	1.0	1.1×10^{-4}	0.75	1
PMT	1.4	1.0	2.7×10^{-4}	1.92	2
PMT	1.4	1.0	3.2×10^{-4}	2.29	3
75/25[b]	800	1.0	1.5×10^{-2}	0.18	1
75/25[b]	800	5.0	1.3×10^{-2}	0.31	1

[a] PMT doped with BF_4^- (rather than the usual $AlCl_4^-$).
[b] Shawinigan-Ketjen blend as described in text.

the electrode in this manner prior to first discharge. In these cycles, recharge was by 0.1 mA cm^{-2} constant current. The first discharge, with BF_4^--doped PMT was very short. On charging, when the 3.8 V cutoff was reached, only 75% of the charge that had been removed was replaced, yet discharge capacity increased nearly threefold (curve B). Replacing 100% required a cutoff potential of 3.88 V, further extending capacity of the subsequent discharge (curve C). "Conditioning" the electrode (undope/dope slowly via constant potential) produced good capacity on first discharge (curve C, Fig 2), whereas several constant current cycles were needed to achieve similar capacity (Figure 3) and anion exchange with an "unconditioned" electrode. Peparing PMT incorporated with $AlCl_4^-$ would eliminate the undoping/doping procedure. We thought this might be possible by performing polymerizations in the presence of either tetrabutylammonium tetrachloroaluminate or lithium tetrachloroaluminate salt. However, these salts were only sparingly soluble in acetonitrile (most of the salt added to prepare a 0.1M solution did not dissolve). Concentrations of dissolved salt were not determined, but on the chance that some dissolution occurred, solution conductivities were measured for comparison against the 0.1 M tetrabutylammonium tetrafluoroborate electrolyte. Conductivities were found to be of the same order of magnitude (Table III), so monomer was added to the supernatant of each solution and used for polymerization of PMT onto glassy carbon rods. Although some polymerization occurred in each electrolyte, coverage and adherence to the substrate were poor, rendering films unsuitable as cathodes.

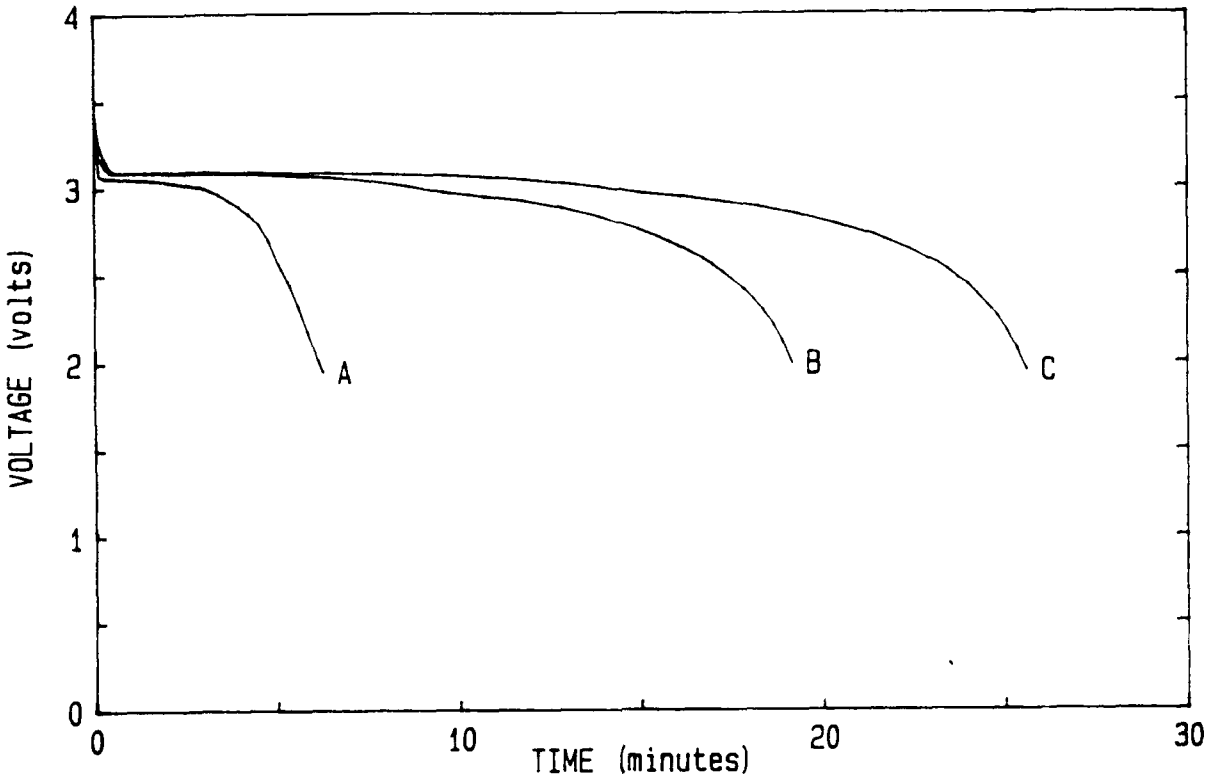

Figure 3. Capacity of 1.4 μm thick PMT at 1 mA cm^{-2} in $Li(SO_2)_3AlCl_4$. First discharge of BF_4^--doped film (A), third (B) and fourth (C) discharges of $AlCl_4^-$-doped film.

TABLE III.
Conductivity of acetonitrile solutions.

Salt in CH_3CN	Molarity	Conductivity S cm^{-1}
Bu_4NBF_4	0.1	9.5×10^{-3}
Bu_4NAlCl_4	<< 0.1	7.7×10^{-3}
$LiAlCl_4$	<< 0.1	8.2×10^{-3}
none	---	3.0×10^{-6}

Usually, cycling of cells was limited to between 10 and 20 cycles. PMT was effectively renewed by recharging at 3.8 V constant potential. Charging cycles which replaced the same numer of coulombs that were removed resulted in identical discharge profiles. Overcharging (by replacing twice the number of coulombs revoved on discharge) increased discharge capacity with no deleterious effects. PMT was very stable on cycling, strongly adhering to the platinum substrate without peeling, flaking, or cracking. In fact, after use, the platinum or glassy carbon substrate had to be abraided with alumina paste in order to remove the polymer film.

In addition to recharge at constant 3.8 V, lower charging potentials were also explored. Figure 4 shows discharge data at 0.1 mA cm^{-2} for PMT that was recharged at 3.7 V constant potential. Cell recharge was nearly as effective as that performed at 3.8 V, although accompanying currents are lower, recharge times longer, and capacity slowly faded with cycling. This lower charging potential further ensures protection from chlorine formation and could be useful for battery applications utilizing trickle charging.

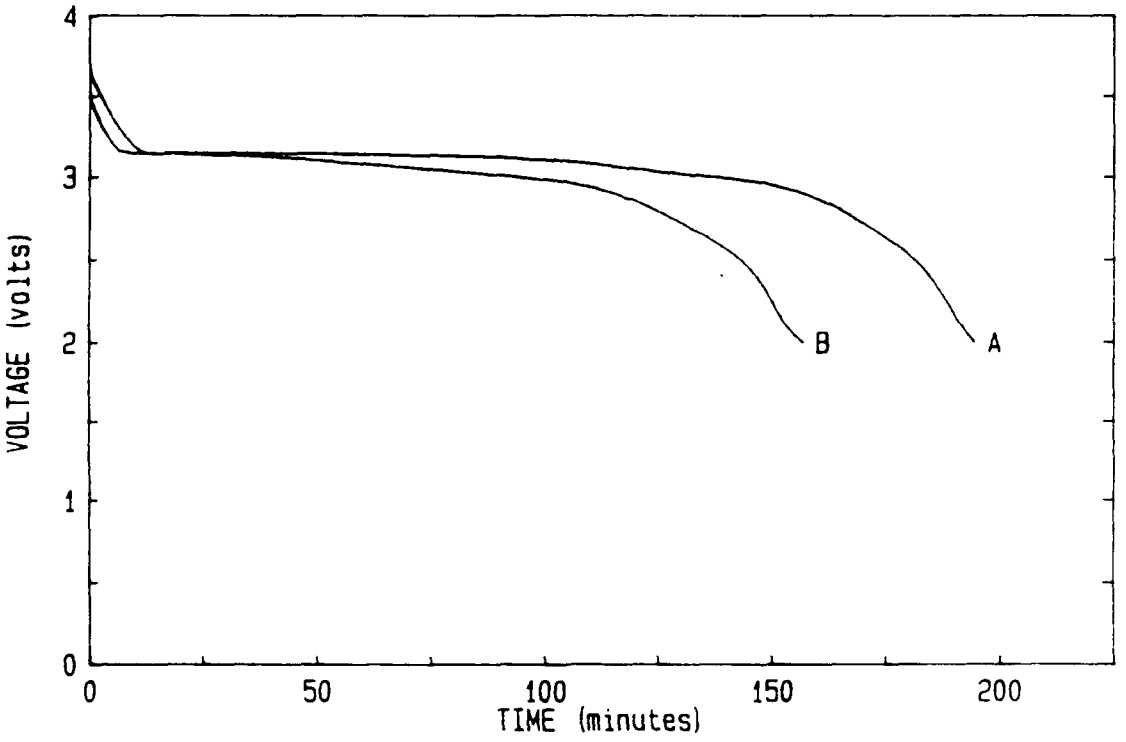

Figure 4. First (A) discharge of 1.4 μm thick PMT at 0.1 mA cm^{-2} and fifth (B) discharge following recharge at 3.7 V constant potential in $Li(SO_2)_3AlCl_4$ electrolyte.

The more common practice of constant current recharge (to a 3.8 V cutoff) was also utilized. In Figure 5, curve A is the first charge (0.1 mA cm^{-2}) of a PMT film initially doped with BF_4^-. Curve B is representative of subsequent charging cycles (films doped with $AlCl_4^-$. Generally, unless lower currents are used, the 3.8 V cutoff was reached (about 150 min) after replacing only 75% of the charge removed on discharge with the 1.4 μm thick films. Replacing 100% of the charge removed during discharge resulted in a final potential at end of charge of between 3.88 and 3.94 V. Three different charging rates for thinner (0.41 μm thick) PMT films are shown in Figure 6. The

shapes of the charging curves are similar to those for 1.4 μm thick films. At the lowest (0.01 mA cm^{-2}) charging rate, cutoff was attained only after very long times. In this case, the low current density and steady voltage approximated a constant potential recharge.

Table II also also summarizes performance data at different discharge rates. Even with the undoping/doping conditioning, the first discharge was often shorter than subsequent cycles because of polymer expansion with cycling. Volumetric energy density of PMT is impressive, exceeding that of PTFE-bonded porous carbon by an order of magnitude at the 1 mA cm^{-2} rate. Performance of the thick blended carbon cathodes agrees with earlier work by Mammone et al. (19), where Shawinigan and Ketjen cathodes discharged at 5 mA cm^{-2} gave 0.22 and 0.42 Ah cm^{-3}, respectively. However, one must bear in mind that the carbon cathodes were much thicker, and if one could prepare a PMT cathode of like thickness, energy density would probably not scale proportionately.

Calvert et al. (20) found that poly(acetylene) had open-circuit voltages and capacities comparable to PTFE-bonded Shawinigan cathodes in lithium sulfur oxyhalide cells. Based on calculated energy density (Ah cm-3) from data for poly(acetylene) in $SOCl_2$ and SO_2Cl_2 (20), our values for the Li/SO_2/PMT system are an order of magnitude higher than those for poly(acetylene).

It should be noted that large porous carbon cathodes containing a blend of Shawinigan and Ketjen blacks (with PTFE binder) could also be successfully recharged at 3.7 or 3.8 V. This seems inconsistent with the recharge mechanisms employing chlorine (1,2).

Recharge which occurs over very long time periods is aided by dissolution of discharge products. After discahrge of a PMT electrode, a subsequent discharge without first recharging the electrode provided no capacity. However, electrodes that were allowed to stand at open circuit for up to 3.5 days showed up to 25% capacity recovery without recharge. Mammone and Binder (1) also observed some recovery of capacity on passivated glassy carbon electrodes allowed to stand at open circuit. The large energy densities observed at very low (0.05 mA cm^{-2}) discharge rates may be explained not only by more complete cathode utilization but also by a concomitant dissolution of product.

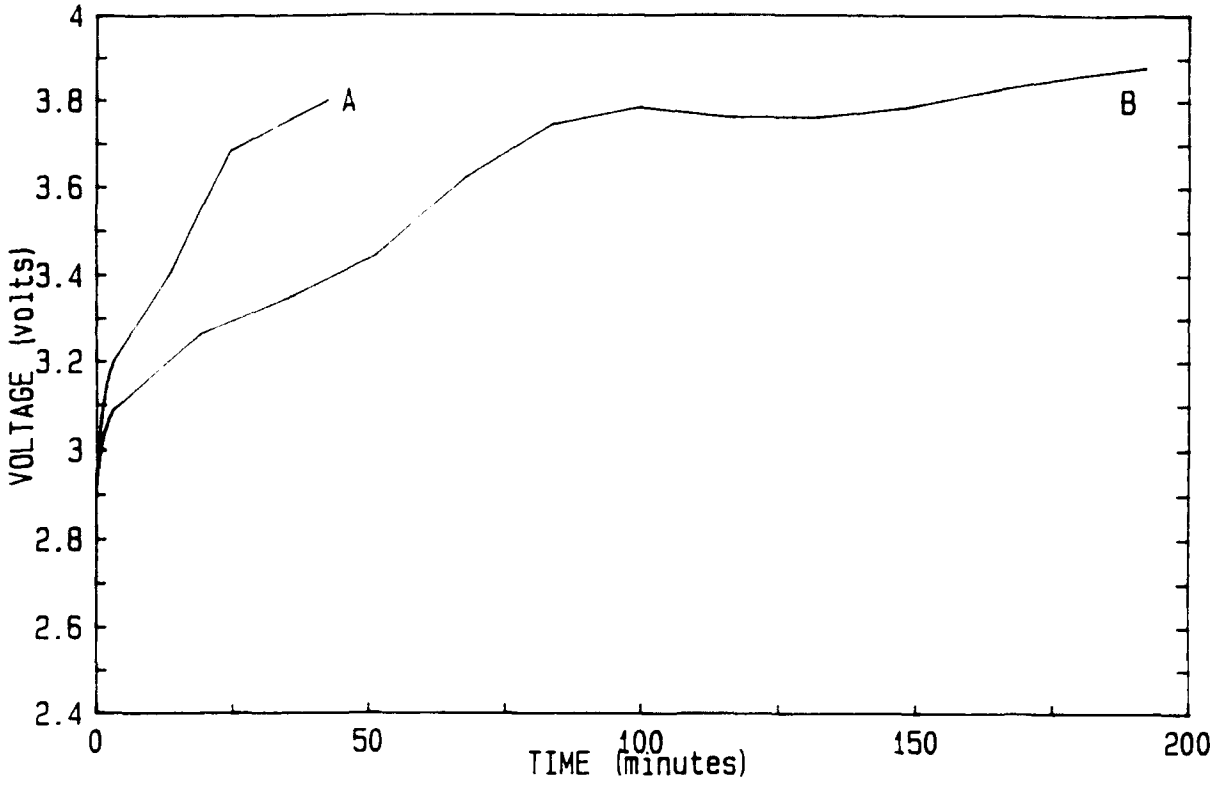

Figure 5. Constant current recharge of $Li/Li(SO_2)_3AlCl_4/1.4\ \mu m$ PMT cell at 0.1 mA cm^{-2} following 1.0 mA cm^{-2} discharge to 2.0 V. Recharge of a film initially doped with BF_4^- (A), and films doped with $AlCl_4^-$ (B).

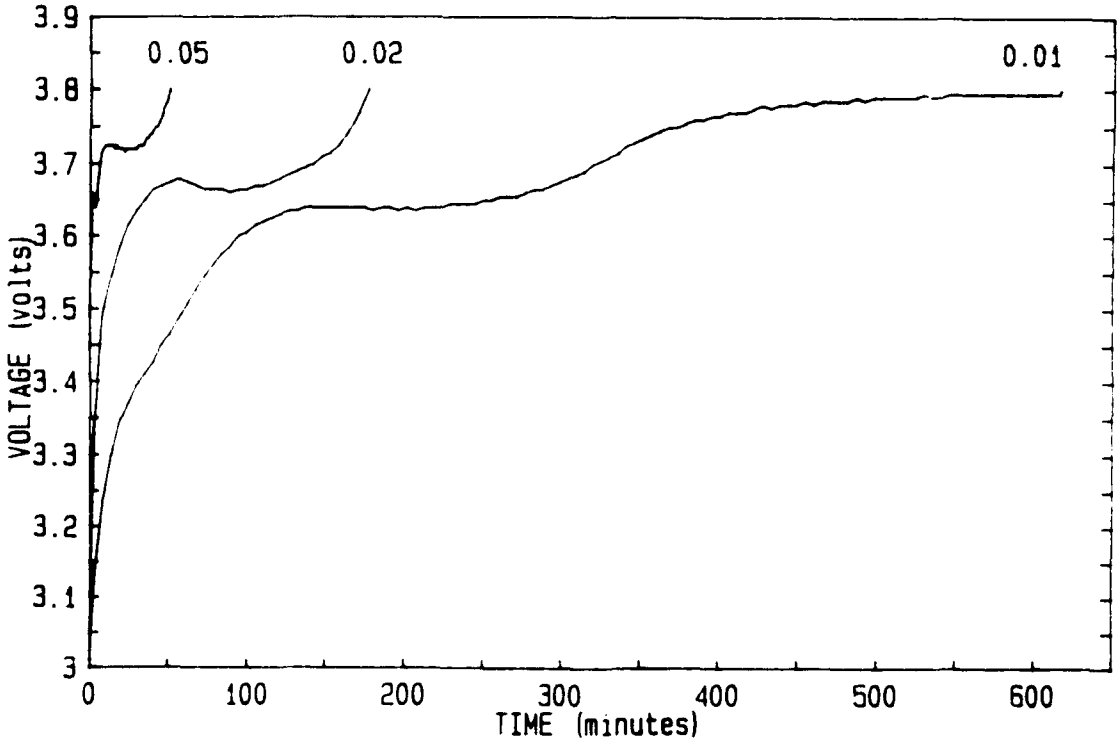

Figure 6. Constant current recharge of $Li/Li(SO_2)_3AlCl_4/0.41\ \mu m$ PMT cell to 3.8 V cutoff at 0.01, 0.02, and 0.05 mA cm^{-2} following 0.5 mA cm^{-2} discharge to 2.0 V.

Dissolution of the discharge product could be explained by the work of Connolly and Thrash (21), which allowed increased solubility of lithium salts (e.g. lithium dithionite) in SO_2 in the presence of quaternary ammonium cations. In our case, product dissolution might be traced to any tetrabutylammonium tetrafluoroborate that may have carried over from the PMT polymerization procedure. Perhaps the addition of small amounts of quarternary ammonium salts could be used for extending discharge capacity.

Pulse Power Discharge - Because pulse power is derived predominantly at the electrode surface (rather than the interior bulk), thin polymer electrodes are both efficient and well suited for bipolar construction employing many electrodes. The high conductivities of $Li(SO_2)_3AlCl_4$ electrolyte and PMT cathodes should minimze cell impedance losses, which are of particular concern for pulse systems.

Three types of experiments were used to evaluate the rate capability of thin PMT films. First, pulse discharge was performed by stepping cell potential cathodic from open circuit. Also, current pulses were applied to determine the ability of PMT to accommodate high constant currents repetitively over pulse periods of several seconds. Lastly, high rate constant current discharges were performed to assess the ability of PMT to perform as a reserve cell.

Potential step pulses - The delivered current was measured at either 2 or 100 μs intervals for up to five seconds following the applied pulse with a Nicolet model 4094C digital oscilloscope. Potentials $\leq$ 2.6 V are more cathodic than the main reduction peak observed for $Li(SO_2)_3AlCl_4$ by cylic voltammetry, ensuring the simultaneous reduction of both the electrolyte and PMT. Based on the maximum mass (4.52×10^{-8} kg) of PMT polymerized, theoretical capacity due to complete polymer undoping from the 35% level would be 2.69×10^{-6} Ah. However, this would not be possible since PMT would become electrically insulating before all of this charge could be removed. Constant current discharge at 1.0 mA cm^{-2} showed that PMT delivered a capacity of 5.3×10^{-5} Ah, which is 20 times greater than expected if capacity were due to undoping alone. Based on this, we assume that the majority of pulse discharge capacity was derived from reduction of the SO_2 electrolyte.

Figure 7 compares current density as a function of the inverse square root of time during the first 13 ms following a potential step from open circuit with 1.4 μm thick PMT and 25 μm thick porous carbon electrodes. Stepping the potential to 2.0 V, PMT delivered more than twice the current ($\approx$ 1130 mA cm^{-2}) as did porous carbon ($\approx$ 480 mA cm^{-2}), achieving over 2 W cm^{-2} for nearly 100 μs. When PMT was pulsed only to 2.6 V, current density remained about 50% higher than that obtained with porous carbon

for up to 400 μs. Again, the superior performance of PMT cannot be explained as an artifact of surface area.

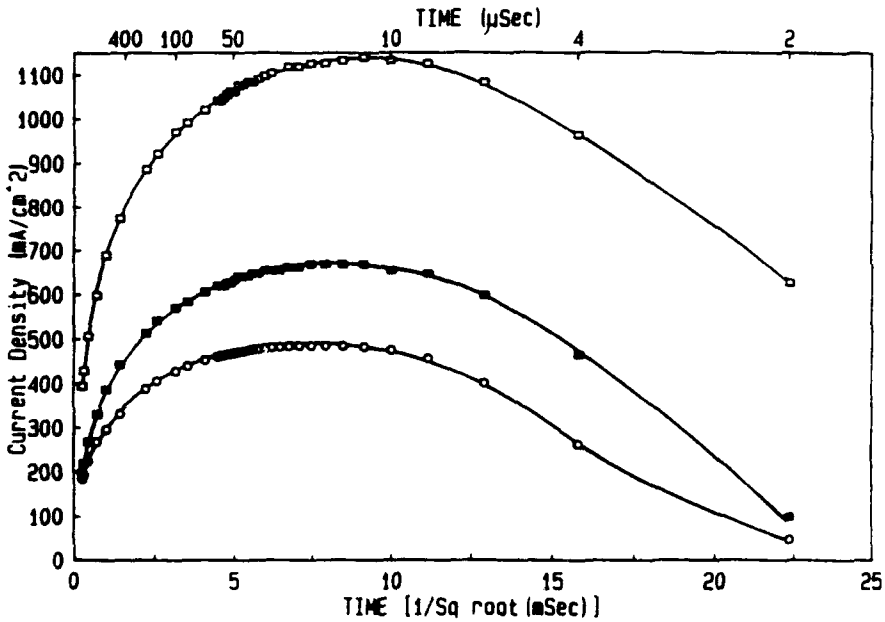

Figure 7. Current density as a function of the inverse square root of time (up to 13 ms) following a potential step from open circuit in a cell containing a Li anode and $Li(SO_2)_3AlCl_4$ electrolyte. Cathodes were 1.4 μm thick PMT stepped to 2.0 V (open square) and 2.6 V (solid square), and 25 μm thick Shawinigan carbon cathode (circle) stepped to 2.0 V.

Bare platinum or glassy carbon electrodes (not shown) delivered approximately 800 mA cm^{-2} for up to 10 μs when stepped to 2.0 V, but currents rapidly fell thereafter. The first few μs after pulsing reflected the contribution due to double layer capacitance, and the period following this indicated the maximum current that could be contributed from electrolyte reduction on the substrate. Thus, any current that might arise from reduction processes on the substrate would be very small and short-lived.

Power (and current) density for up to 0.5 s following a potential step from OCV to 2.0 V is shown in Figure 8. Almost no current arises from the glassy carbon (or platinum) substrate beyond 10 ms, indicating again that any current contributed from the substrate was negligible. Although 25 μm thick porous electrodes provided 20 mA cm^{-2} out to 0.5 s, PMT delivered nearly three times the current (56 mA cm^{-2}) and power density of 800 W cm^{-3} at 0.5 s. In a smaller potential step to 2.6 V (not shown), PMT delivered 42 mA cm^{-2} (780 W cm^{-3}) after 0.5 s. Total charge delivered during potential steps to 2.6 V and 2.0 V is given for several time periods in Figures 9 and 10. PMT was able to deliver more than twice the charge of porous carbon up to 500

ms. Although the total charge passed by PMT was higher for the 2.0 V pulse, power density after 0.5 s was similar for pulses to 2.0 V and 2.6 V (800 and 780 W cm^{-3} respectively). This indicates that by 0.5 s the discharge process is largely diffusion limited, and larger pulses will not result in significantly more power. So for a relatively long (0.5 s) pulse period, a shallow pulse to 2.6 V is sufficient, and also allows PMT to be more easily recharged than if it were discharged to lower potentials.

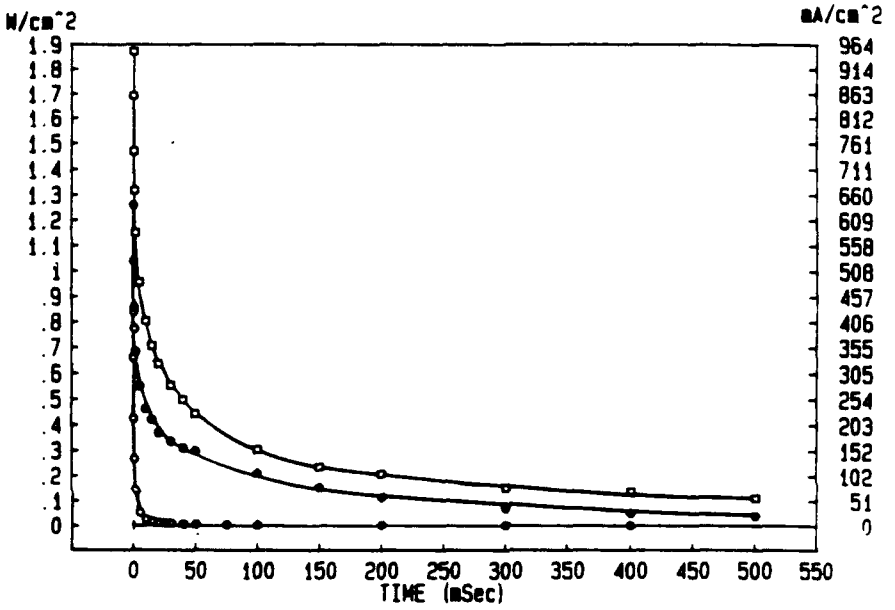

Figure 8. Power and current density as a function of time for up to 0.5 s after a potential step from open circuit to 2.0 V. Cathodes were 1.4 μm thick PMT (open square), 25 μm thick Shawinigan carbon (solid circle), and glassy carbon (open circle).

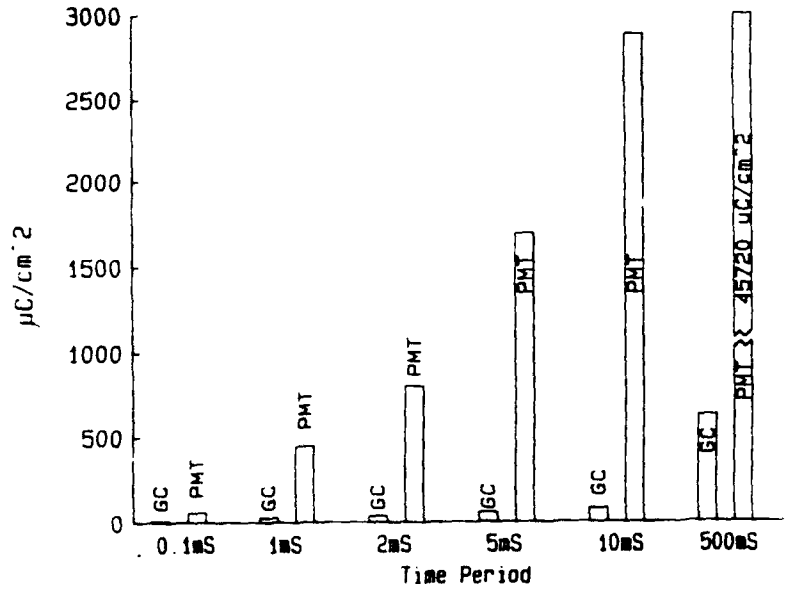

Figure 9. Total charge delivered over various time periods for glassy carbon (GC) and 1.4 µm thick PMT cathodes in $Li(SO_2)_3AlCl_4$ electrolyte, stepped from open circuit to 2.6 V.

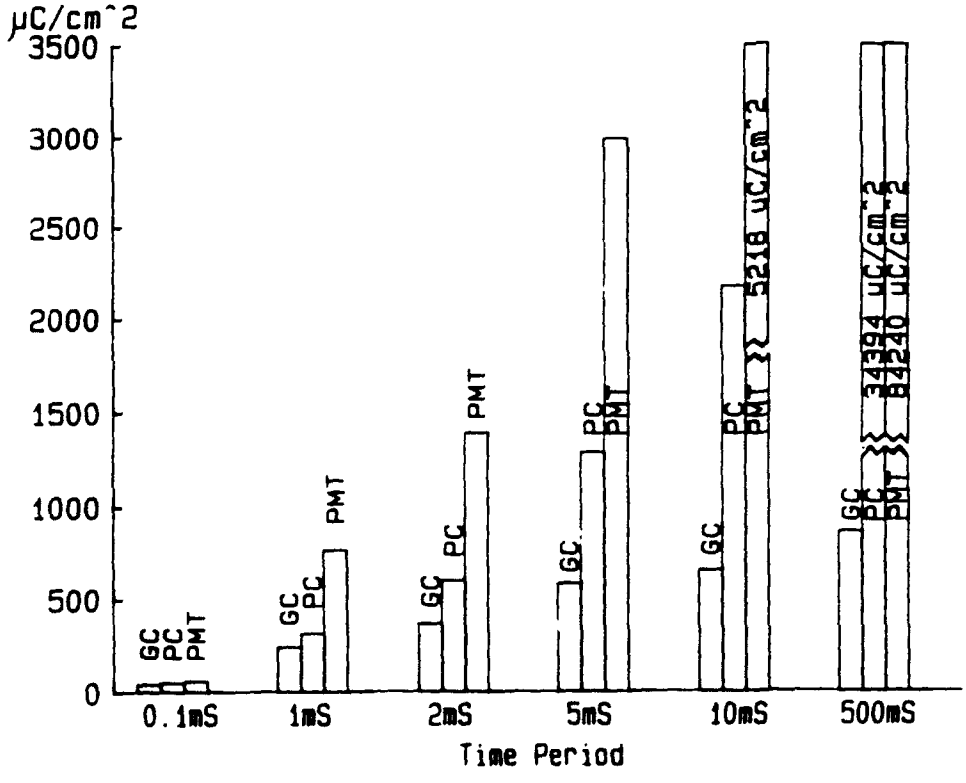

Figure 10. Total charge delivered over various time periods for glassy carbon (GC), 25 µm thick Shawinigan porous carbon (PC), and 1.4 µm thick PMT cathodes in $Li(SO_2)_3AlCl_4$ electrolyte, stepped from open circuit to 2.0 V.

In Table IV, current and power density (potential step to 2.6V) are shown for up to five seconds. Very high current densities (>100 mA cm^{-2}) occurred during the first second, however, currents fell to 26 mA cm^{-2} (≈0.07 W cm^{-2}, 489 W cm^{-3}) after five seconds. Although mass transport limits the ability to sustain high power for longer periods, these short-lived high power pulses might be suitable for pulse applications, by configuring many cells in a bipolar stack.

TABLE IV.
Current and power density over time for 1.4 μm thick PMT in $Li(SO_2)_3AlCl_4$ electrolyte stepped from OCV to 2.6 V.

Elapsed Time (Seconds)	Current Density (A cm-2)	Power Density (W cm-2)
0.001	0.723	1.880
0.01	0.479	1.245
0.1	0.273	0.710
1.0	0.126	0.328
2.0	0.063	0.164
3.0	0.041	0.107
4.0	0.033	0.086
5.0	0.026	0.068

Thicker PMT electrodes containing twice the amount of material used to form the 1.4 μm thick film were also pulsed, but measured currents were the same as for the 1.4 μm thick PMT. Further, constant current discharge capacity of these thicker films showed only marginal improvement, so it was concluded that PMT films thicker than 1.4 μm offer no advantage.

Constant current pulses - PMT was also evaluated for intermittent constant current pulse power capability. A constant current load was applied for four seconds, and cell potential measured at the end of this period. Following a one second rest at open circuit, the cell was pulsed again. This procedure was repeated until cell potential fell below 2.0 V. The cell was then recharged at 0.2 mA cm^{-2} to a 3.8 V cutoff, after which the next cycle was begun. Figure 11 shows the final potential and power density when PMT was discharged at 15 mA cm^{-2}. PMT was pulse discharged for twenty one cycles (arbitrary number of cycles), with each cycle providing eight pulses. Except for the last pulse in each set, final potentials were remarkably similar even after 21 cycles. During the first six pulses, the final potential ranged between 3.0 V on the first pulse and 2.7 V on the sixth pulse, corresponding to power densities of 0.045 and 0.040 W cm^{-2} (321 and 289 W cm^{-3}) respectively. At a 25 mA cm^{-2} rate, Figure 12, four to five pulses were obtained for 35 cycles.

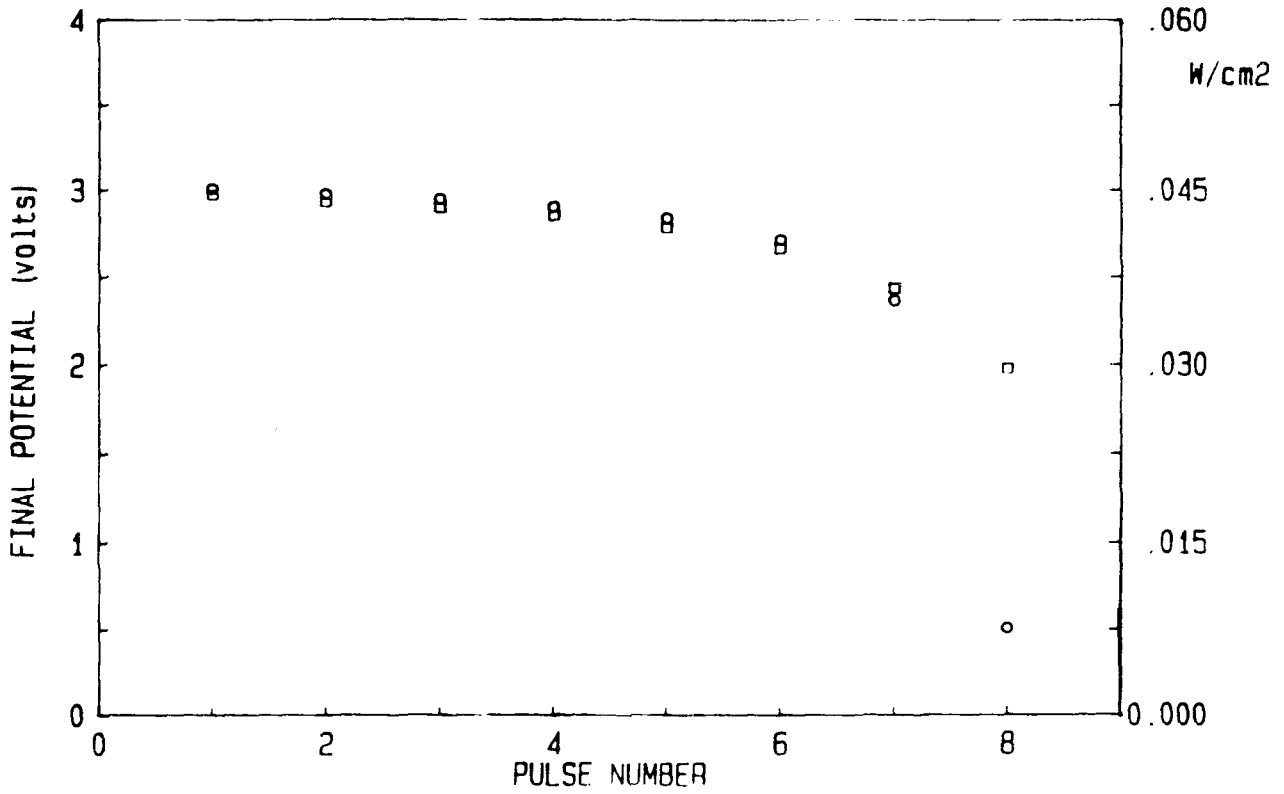

Figure 11. Final potential of $Li/Li(SO_2)_3AlCl_4/1.4$ μm PMT cell after each 4 second, 15 mA cm^{-2} pulse, with 1 second open circuit rest periods between pulses. Recharge was at 0.2 mA cm^{-2} to a 3.8 V cutoff. First (square) and 21st (circle) pulse sets.

Only the first three pulses were reproducible, with final potentials between 2.9 and 2.6 V, and power densities of 518 to 464 W cm^{-3} respectively. At 50 mA cm^{-2}, PMT was able to deliver only one or two pulses to cutoff. These experiments demonstrated the ability of PMT to deliver several pulses over a short time period, and then to be reproducibly repeated for several cycles.

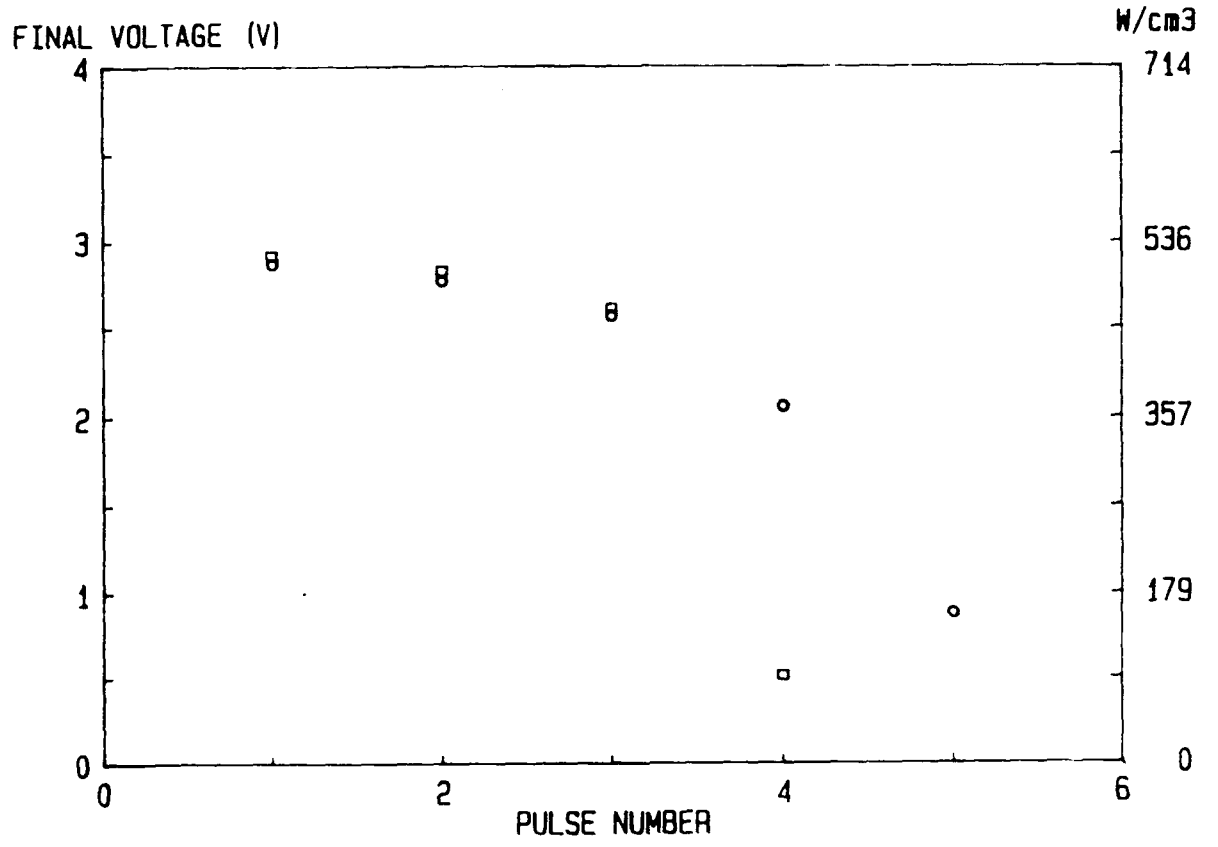

Figure 12. Final potential of $Li/Li(SO_2)_3AlCl_4/1.4$ μm PMT cell after each 4 second, 25 mA cm^{-2} pulse, with 1 second open circuit rest periods between pulses. Recharge was at 0.2 mA $^{-2}$ to a 3.8 V cutoff. Second (square) and 35th (circle) pulse sets.

High rate constant current discharge - High rate discharge characteristics of PMT in other inorganic electrolytes was also investigated, conceivably for use in a reserve cell. Constant current discharges were performed in 1.0 M $LiAlCl_4$-$SOCl_2$, 1.0 M $LiAlCl_4$-SO_2Cl_2, and $Li(SO_2)_3AlCl_4$ at 10, 20, and 30 mA cm^{-2}. In the SO_2-based electrolyte, PMT was "conditioned" as previously described prior to discharge. Cells with $SOCl_2$ (3.55 OCV) and SO_2Cl_2 3.83 OCV) electrolytes were used as non-rechargable cells, so a fresh BF_4^--doped PMT electrode was required for each run. To increase the dopant level we tried holding cell potential at 3.8 V for 30 minutes in the thionyl chloride-based electrolyte, presumedly further doping the PMT with $AlCl_4^-$. Although the charge delivered from polymer undoping is insignificant compared to that derived from electrolyte reduction, we surmised that this doping process might favorably alter structural and performance characteristics (as is observed in SO_2 electroltye). However, no change in performance was observed, inidicating that at high rates of discharge, the dopant anion and level of doping have little effect on discharge capacity in $SOCl_2$ electrolyte.

Operating potential and volumetric power density are shown for constant current discharge in Figures 13-15, and Table V

summarizes the average energy densities. Bare platinum and bare glassy carbon control electrodes gave no capacity at the 10 mA cm^{-2} rate in thionyl chloride. In fact, at 1 mA cm^{-2}, only 0.8 minutes of dishcarge was obtained to a 2.0 V cutoff.

Although the sulfuryl chloride electrolyte provided the highest operating potential during the initial part of a discharge, the thionyl chloride-based electrolyte delivered the highest cell capacity at all current densities. Also, operating potential was most constant in the $SOCl_2$ electrolyte. Lowest operating potential and shortest discharge times were observed in the SO_2-based electrolyte (Figures 13 and 14). At the 20 mA cm^{-2} rate (Figure 2), PMT in $SOCl_2$ discharged for nearly two minutes at an operating potential of 3.0 V and 429 W cm^{-3} power density. At 30 mA cm^{-2} (Figure 3), PMT delivered about 600 W cm^{-3} at a potential of 3.0 V in both $SOCl_2$ and SO_2Cl_2 for at least 0.5 minutes. At the 10 and 20 mA cm^{-2} discharge rates, PMT in $SOCl_2$ had a capacity of about 1.1 Ah g^{-1} (Table V). This is comparable to the results reported by Calvert et al. (20) for 50 to 330 fm thick films of poly(acetylene) in $SOCl_2$. In flooded cells, at discharge rates of 12.5 and 25 mA cm^{-2}, they observed capacities of 1.37 and 1.06 Ah g^{-1} respectively.

Compared to the oxyhalide electrolytes, constant current discharge in SO_2 electrolyte is poor at high current densities. However, this electrolyte affords rechargeability, and can accommodate short pulses at high currents for many cycles (Figures 11 and 12).

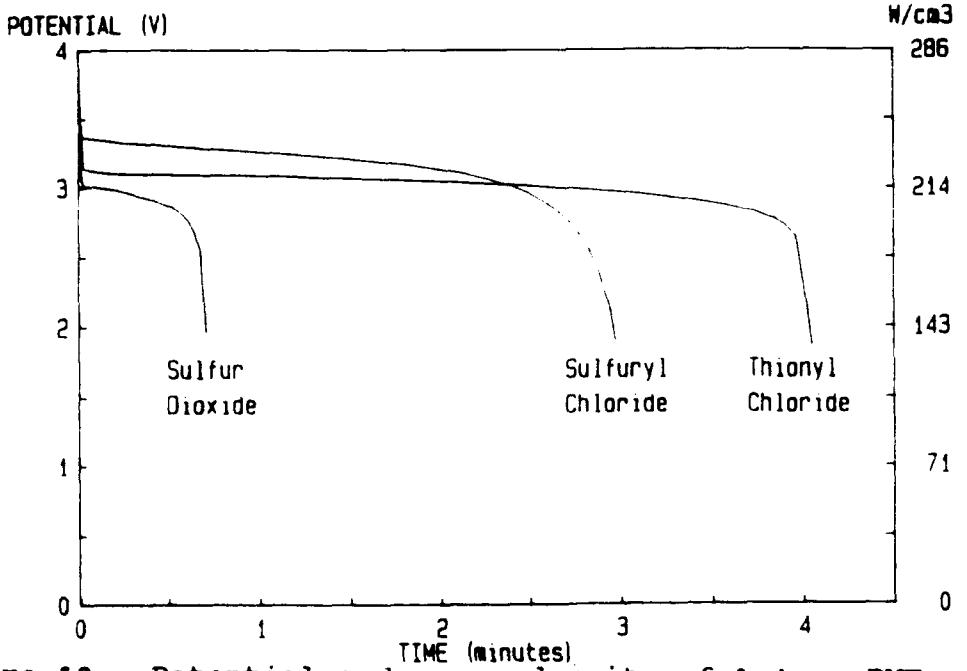

Figure 13. Potential and power density of 1.4 μm PMT as a function of discharge time at 10 mA cm^{-2} constant current in various electrolytes.

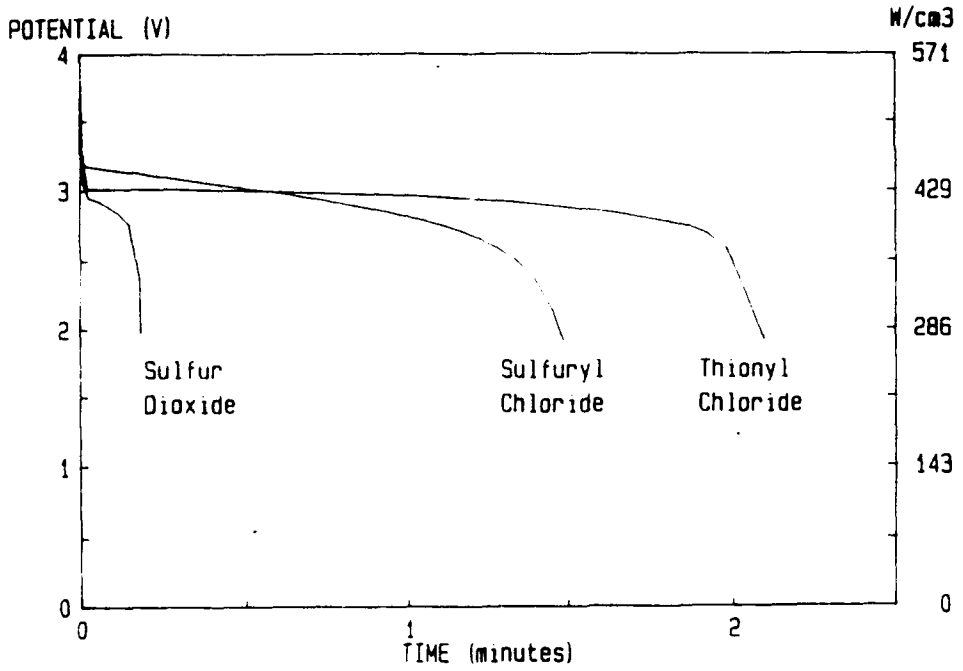

Figure 14. Potential and power density of 1.4 μm PMT as a function of discharge time at 20 mA cm^{-2} constant current in various electrolytes.

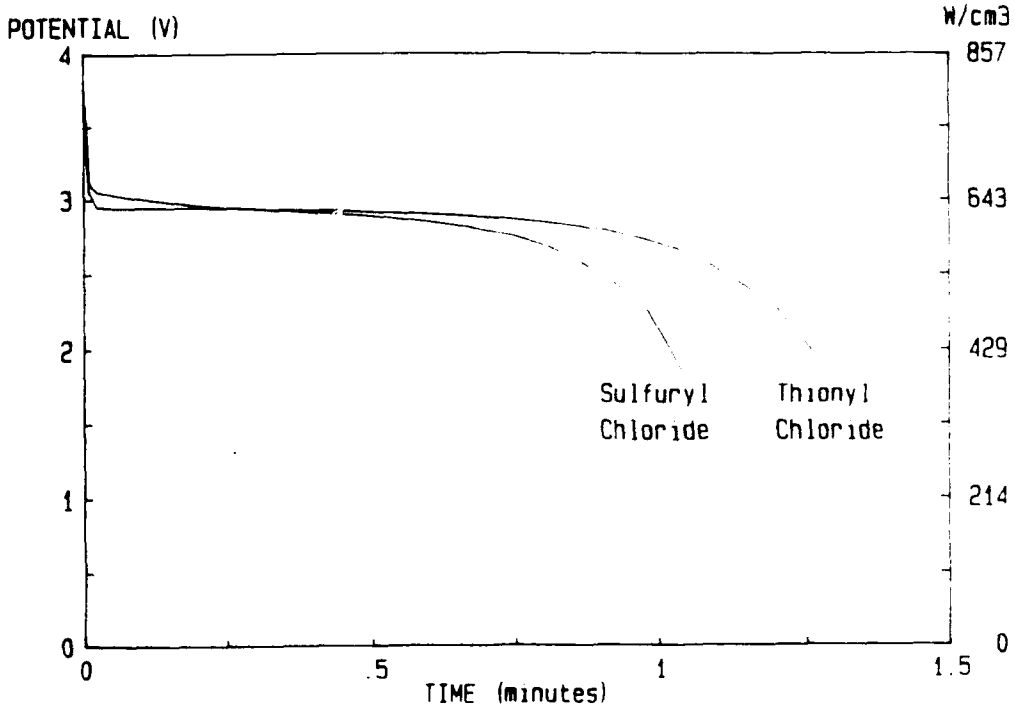

Figure 15. Potential and power density of 1.4 μm PMT as a function of discharge time at 30 mA cm^{-2} constant current in various electrolytes.

TABLE V.
Capacity of 1.4 μm thick PMT at various discharge rates in SO_2, $SOCl_2$, and SO_2Cl_2 electrolytes.

Solvent	Rate mA cm^{-2}	Capacity minutes	Ah g^{-1}	mAh cm^{-2}	Ah cm^{-3}
SO_2	10	0.72	0.189	0.120	0.857
	20	0.20	0.105	0.067	0.476
SOCl2	10	4.1	1.075	0.683	4.883
	20	2.1	1.101	0.700	5.002
	30	1.25	0.983	0.625	4.466
SO_2Cl_2	10	3.04	0.797	0.507	3.621
	20	1.54	0.807	0.513	3.668
	30	1.03	0.810	0.515	3.680

CONCLUSIONS

PMT films can be used as rechargeable electrodes in SO_2-based electrolyte, performing better than porous carbon electrodes of comparable thickness. Although surface area of PMT is less than that of porous carbons, constant current discharge capacity of thin electrodes is much greater. Because PMT can be recharged at potentials as low as 3.7 V, corrosion associated with the formation of chlorine can be minimized, which should extend cell life.

Good pulse power characteristics make PMT a feasible candidate for a high power battery system. Very thin films of PMT were able to sustain power levels of at least 2 W cm^{-2} for 100 μs, and 0.1 W cm^{-2} after 0.5 s. Constant current four-second pulses of 25 mA cm^{-2} were reproducible over many cycles, providing four or five pulses (to a 2.0 V cutoff). At 15 mA cm^{-2}, eight pulses were obtained to cutoff. Since PMT is easily electropolymerized onto a current collector, it could readily be incorporated into a bipolar cell design.

Considering the use of PMT in a reserve cell, electrolytes other than $Li(SO_2)_3AlCl_4$ are more suitable for high rate constant current dishcarge. A 1.0 M $LiAlCl_4$ electrolyte in either $SOCl_2$ or SO_2Cl_2 gave considerably more capacity, $SOCl_2$ electrolyte being superior. With thionyl chloride, a load of 30 mA cm^{-2} was sustained for 1.25 minutes to a 2.0 V cutoff. At 10 mA cm^{-2}, over four minutes of capacity was obtained.

An advantage of using electrically conductive polymers is that when they are reduced to the neutral state, they become electrically insulating. This could act as a built-in safety

mechanism to prevent over-discharge abuse. This is an attractive feature when contemplating the production of high energy batteries to deliver high power.

REFERENCES

1. R. J. Mammone and M. Binder, J. Electrochem. Soc., 133, 1312 (1986).

2. A. N. Dey, H. C. Kuo, D. Foster, C. Schleikjer, and M. Kallianidis, "Proceedings of the 32nd Power Sources Conference," June 9-12, 1986. The Electrochemical Society, Inc., p. 176.

3. A. Yassar, J. Roncali, and F. Garnier, Macromolecules, 22, 804 (1989).

4. G. Tourillon and F. Garnier, J. Phys. Chem., 87, 2289 (1989).

5. T. Nagatomo and O. Omoto, J. Electrochem. Soc., 135, 2124 (1988).

6. C. W. Walker, Jr., W. Wade, Jr., M. Binder, and S. Gilman, J. Electrochem. Soc., 132, 1536 (1985).

7. C. W. Walker, Jr., U. S. Patent 4,988,588, January 29, 1991.

8. J. R. Reynold, S. G. Hsu, and H. J. Arnott, J. Polym. Sci. Part B Polym. Phys., 27, 2081 (1989).

9. T. Nagatomo, M. Mitsui, D. Matsutani, and O. Omoto, Trans. IEICE, E70, 346 (1987).

10. M. Ito, A. Tsuruno, S. Osawa, and K. Tanaka, Polymer, 29, 1161 (1988).

11. W. Zhang and S. Dong, J. Electrochem. Soc., 284, 517 (1990).

12. R. J. Mammone and M. Binder, J. Electrochem. Soc., 135, 1057 (1988).

13. W. K. Behl, In "Proceedings of the 27th Power Sources Conference," June 24-26, 1976. The Electrochem. Soc. Inc., p. 30.

14. W. K. Behl, J. Electrochem. Soc., 127, 1444 (1980).

15. C. W. Walker, Jr., J. Electrochem. Soc., 138, 1559 (1991).

16. D. Ofer, R. M. Crooks, and M. S. Wrighton, J. Amer. Chem. Soc., 112, 7869 (1990).

17. T. Kawai, T. Kuwabara, S. Wang, and K. Yoshino, J. Electrochem. Soc., 137, 3793 (1990).

18. F.-J. Pern and A. J. Frank, J. Electrochem. Soc., 137, 2769 (1990).

19. R. Mammone, S. Gilman, and M. Binder, "Proceedings of the 32nd Power Sources Conference," June 9-12, 1986. The Electrochem. Soc., Inc. p. 143.

20. J. M Calvert, B. Weiner, J. Smith, and R. Nowak, J. Electrochem. Soc., 136, 593, (1989).

21. J. F. Connolly and R. J. Thrash, U. S. Patent 4,482,616, November 13, 1984.

ELECTRONICS TECHNOLOGY AND DEVICES LABORATORY
MANDATORY DISTRIBUTION LIST
CONTRACT OR IN-HOUSE TECHNICAL REPORTS

101 Defense Technical Information Center*
ATTN: DTIC-FDAC
Cameron Station (Bldg 5)
Alexandria, VA 22304-6145
(*Note: Two copies for DTIC will be sent from STINFO Office.)

483 Director
US Army Material Systems Analysis Actv
ATTN: DRXSY-MP
001 Aberdeen Proving Ground, MD 21005

563 Commander, AMC
ATTN: AMCDE-SC
5001 Eisenhower Ave.
001 Alexandria, VA 22333-0001

609 Commander, LABCOM
ATTN: AMSLC-CG, CD, CS (In turn)
2800 Powder Mill Road
001 Adelphi, Md 20783-1145

612 Commander, LABCOM
ATTN: AMSLC-CT
2800 Powder Mill Road
001 Adelphi, MD 20783-1145

620 Commander,
US Army Laboratory Command
Fort Monmouth, NJ 07703-5000
1 - SLCET-DD
2 - SLCET-DT (M. Howard)
1 - SLCET-DR-B
35 - Originating Office

681 Commander, CECOM
R&D Technical Library
Fort Monmouth, NJ 07703-5000
1- ASQNC-ELC-I-T (Tech Library)
3- ASQNC-ELC-IS-L-R (STINFO)

705 Advisory Group on Electron Devices
ATTN: Documents
2011 Crystal Drive, Suite 307
002 Arlington, VA 22202

ELECTRONICS TECHNOLOGY AND DEVICES LABORATORY
SUPPLEMENTAL CONTRACT DISTRIBUTION LIST
(ELECTIVE)

205 Director
Naval Research Laboratory
ATTN: CODE 2627
001 Washington, DC 20375-5000

221 Cdr, PM JTFUSION
ATTN: JTF
1500 Planning Research Drive
001 McLean, VA 22102

301 Rome Air Development Center
ATTN: Documents Library (TILD)
001 Griffiss AFB, NY 13441

437 Deputy for Science & Technology
Office, Asst Sec Army (R&D)
001 Washington, DC 20310

438 HQDA (DAMA-ARZ-D/Dr. F.D. Verderame)
001 Washington, DC 20310

520 Dir, Electronic Warfare/Reconnaissance
Surveillance and Target Acquisition Ctr
ATTN: AMSEL-EW-D
001 Fort Monmouth, NJ 07703-5000

523 Dir, Reconnaissance Surveillance and
Target Acquisition Systems Directorate
ATTN: AMSEL-EW-DR
001 Fort Monmouth, NJ 07703-5000

524 Cdr, Marine Corps Liaison Office
ATTN: AMSEL-LN-MC
001 Fort Monmouth, NJ 07703-5000

564 Dir, US Army Signals Warfare Ctr
ATTN: AMSEL-SW-OS
Vint Hill Farms Station
001 Warrenton, VA 22186-5100

602 Dir, Night Vision & Electro-Optics Ctr
CECOM
ATTN: AMSEL-NV-D
001 Fort Belvoir, VA 22060-5677

603 Cdr, Atmospheric Sciences Lab
LABCOM
ATTN: SLCAS-SY-S
001 White Sands Missile Range, NM 88002

607 Cdr, Harry Diamond Laboratories
ATTN: SLCHD-CO, TD (In turn)
2800 Powder Mill Road
001 Adelphi, MD 20783-1145